Electronic Supplementary Information

Multiplexed arrays of chemosensors by parallel dip-pen nanolithography

Alberto Martínez-Otero,[a] *Pablo González-Monje,*[a] *Daniel Maspoch,*[a] *Jordi Hernando**[b] *and Daniel Ruiz-Molina**[a]

[a] Centro de Investigación en Nanociencia y Nanotecnología (CIN2, ICN-CSIC), Esfera UAB, 08193 Cerdanyola del Vallès, Spain

[b] Departament de Química, Universitat Autònoma de Barcelona, 08193 Cerdanyola del Vallès, Spain

jordi.hernando@uab.es, dani.ruiz@cin2.es

1) Materials and methods for DPN preparation of multiplexed arrays of fluorescent pH indicators

Materials: N-(6-aminohexyl)-aminopropyltrimethoxysilane (AHAPS) was purchased from Gelest , whereas anhydrous toluene, acetonitrile, butyl isothiocyanate, dimethylformamide, ethanol, sodium acetate buffer solution (3M, pH 5.2), phosphate buffer solution (PBS) (1M, pH 7.4) and glycerol were purchased from Sigma-Aldrich. Borax Buffer Solution (13 mM, pH 9.0) was purchased from Fluka. The amino-reactive fluorescent dyes Oregon Green 514 succinimidyl ester (OG), fluorescein isothiocyanate (FL) and carboxynaphtofluorescein succinimidyl ester (NF) were purchased from Invitrogen. In Table S1 a summary of the pH-dependent optical properties of these dyes is given and their molecular structures are shown in Figure S1.

Table S1 pH-dependent optical properties of free OG, FL and NF in aqueous solution.

Molecule		λ_{abs} [nm]	λ_{em} [nm]	Φ_f	pKa
OG[a]	pH 9	508	528	0.65	4.7
	pH 3	492, 463	524	0.22	
FL[b]	pH 9	494	522	0.93	6.4, 4.3
	pH 5.5	478, 460	519	0.37	
	pH 3	440	519[c]	0	
NF[d]	pH 10	598	670	-	7.6
	pH 5.5	512	572	-	

[a] Fluorescence quantum yields and pKa from ref. 1.

[b] Fluorescence quantum yields are given for the most abundant protonation states of fluorescein at each pH value: dianionic (pH 9), anionic (pH 5.5) and neutral (pH 3) states. Φ_f and pKa values from ref. 2.

[c] Excited-state deprotonation of the neutral form of fluorescein results in emission from its neutral excited state.[2]

[d] Data for naphtofluorescein from ref. 3.

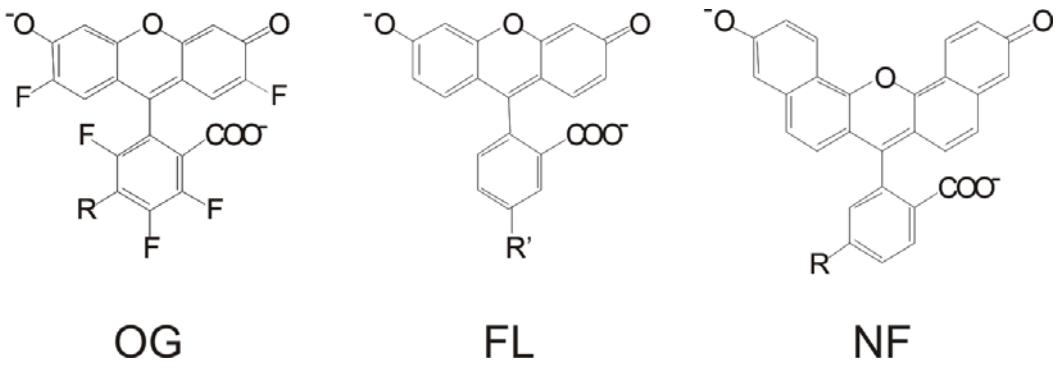

Fig. S1 Molecular structures at pH 9.5 of the derivatives of Oregon Green® 514 (OG), fluorescein (FL) and 5-carboxynaphtofluorescein (NF) used in this work. R and R' stand for the amino-reactive succinimidyl ester and isothiocyanate groups, respectively.

Substrate preparation: Aminosilane self-assembled monolayers were prepared onto glass slides of ~120 μm in thickness (VWR Scientific), which were previously cleaned for 15 min in piranha solution (Caution: *Piranha solution is an extremely strong oxidant and should be handled very carefully!*). After rinsing with high purity water and drying in a stream of nitrogen, the freshly cleaned glass slides were immersed in a 2% (w/w) AHAPS solution in anhydrous toluene for 4 h under dry conditions in a glove box. Subsequently, the slides were sonicated in anhydrous toluene, ethanol and deionised water to remove any physisorbed material and, finally, they were rinsed with high purity water and dried in a stream of nitrogen just prior to DPN-patterning.

DPN-patterning: DPN experiments were carried out with a commercial Dip Pen writer called NSCRIPTOR™ DPN® System (NanoInk Inc., USA). Gold-coated commercial 1-D pen arrays with 12 A-frame AFM cantilevers (Si_3N_4, NanoInk, Inc., USA) were used for patterning. The cantilevers are 100 μm long and have force constant of 0.5 N/m. All DPN patterning experiments were carried out under ambient conditions (~ 35% relative humidity, 20-24 ^oC). To load the inks onto the tips, microfluidic ink delivery chip-based systems (Inkwell, NanoInk, Inc., USA) were used, which contain

several reservoirs connected to separate microwells. Three of these reservoirs were filled with around 0.3 μL of the different liquid inks, which consisted of 1 mM solutions of the amino-reactive dyes of interest in 95% dimethylformamide and 5% glycerol. Subsequently, three consecutive tips of the 1-D pen array were coated with the desired inks by dipping them into the microwells. The separation between the microwells prevents any kind of cross-contamination. Finally, the three coated tips were brought into contact to the substrate surface to create nanostructures of OG, FL and NF using a dwell time of 0.4 s. In a single deposition step, the separation between OG, FL and NF nanostructures is determined by the inter-tip separation in the 1-D pen array (~60 μm). To attain shorter separations, consecutive deposition steps can be performed in which tips are moved to the desired positions of the surface, as depicted in Fig. S2.

Treatment of the DPN-patterned substrates: The remaining free amino groups on the surface of the glass substrates after DPN-patterning were finally capped by reaction with a 5% butyl isothiocyanate solution in acetonitrile for 4 hours. Subsequently, the substrates were sonicated in acetonitrile, ethanol and deionised water to remove any physisorbed material and, finally, they were dried in a stream of nitrogen.

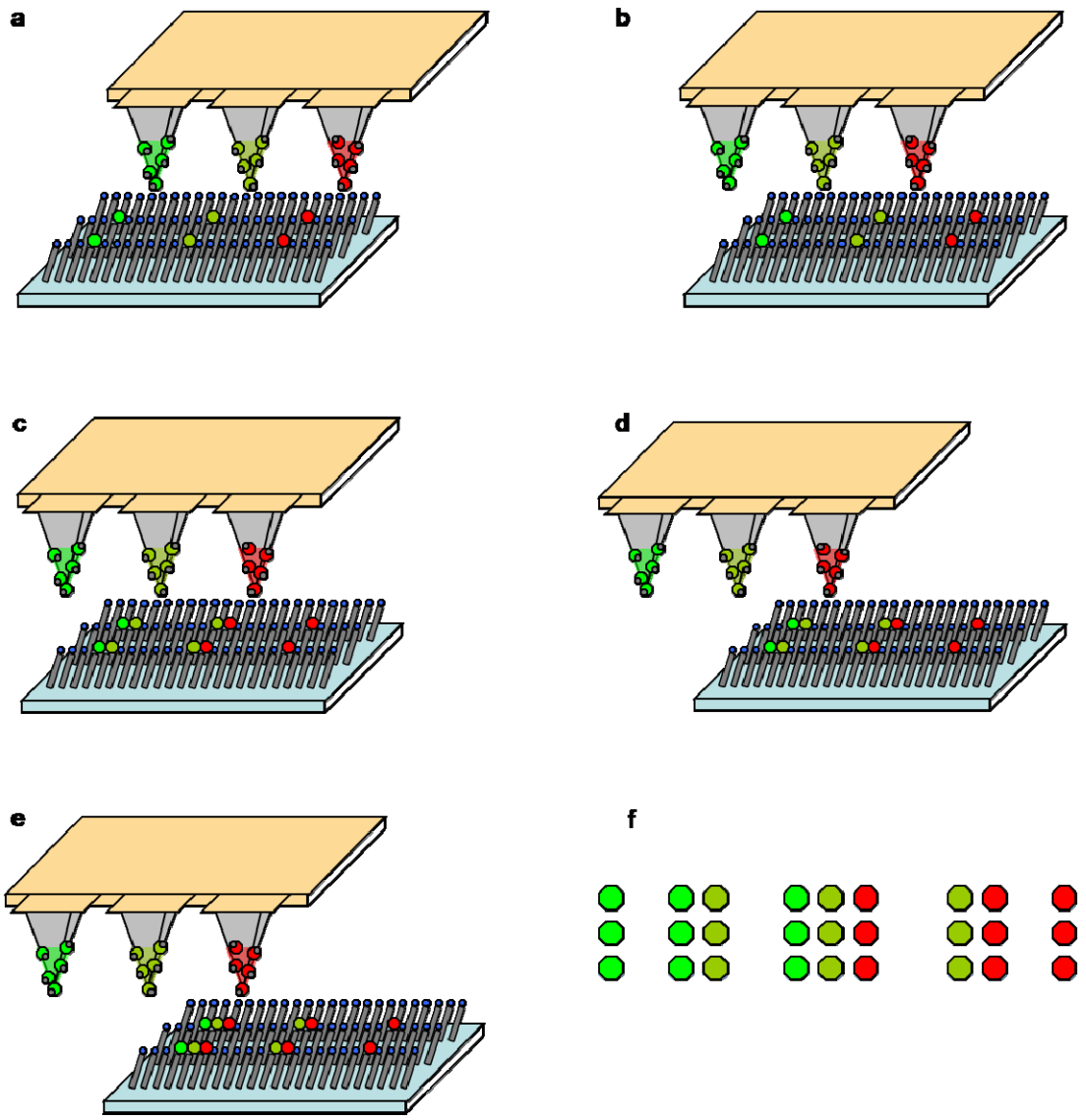

Fig. S2 Schematic representation of the fabrication of multiplexed matrices of OG, FL and NF whose nanostructures are separated by less than the tip-distance (60 μm): (a) first DPN deposition step, which results in OG, FL and NF dots separated by 60 μm; (b) translational movement of the DPN tips; (c) second DPN deposition step, (d) translational movement of the DPN tips; (e) third DPN deposition step. An upper view of the imprinted structures resulting from this multi-step process is depicted in figure (f), which shows that a 3x3 dot matrix of OG, FL and NF with very short inter-dot distances is created. Indeed, the minimum separation between structures of different dyes that can be attained in this way basically depends on the accuracy of the translational movement of the tips.

2) Characterization of the DPN-patterned substrates

Contact angle measurements: Water contact angles on the prepared monolayers were measured by means of the sessile drop shape method under ambient conditions and immediately after surface functionalization. 3 mL of deionized water were dropped onto the monolayer of interest and contact angles were then calculated by the computer software (Drop Shape Analysis DSA 100, Kruss, Germany) provided with the analyzer (Easy Drop FM40, Kruss, Germany). Contact angles on five different regions on each sample were measured and averaged. AHAPS-functionalized glass substrates displayed a contact angle of 60.4º, as expected for amino-terminated self-assembled monolayers.[4] Subsequent DPN-patterning of the AHAPS SAM followed by capping of the remaining free amino groups by reaction with butyl isothiocyanate resulted in an increase of the contact angle to 72.4º, similarly to previously reported.[5]

Atomic force microscopy: All AFM images were recorded on an Agilent 5500 AFM/SPM microscope. The AFM was operated in contact mode. A multi-purpose low-coherence scanner with scan range up to 90 μm was used for imaging samples under ambient conditions. The AFM probes were type NCH silicon pointprobes (force constant ≈ 42 $N.m^{-1}$, resonant frequency ≈ 330 KHz) from Nanosensors (Neuchatel, Switzerland). The scan rate was tuned proportionally to the area scanned and was kept in the 0.5-1.2 Hz range. The typical value of drive amplitude was 1.0-1.4 V. The resolution of image acquisition was 512 pixels per line.

pH measurements: pH measurements with a Crison 5028 pH electrode in a Crison BASIC 20+ potentiometer were performed in situ during the acid/base studies of the DPN-patterned substrates.

Confocal fluorescence microscopy: A home-made confocal scanning fluorescence microscope with a homebuilt liquid-chamber was used for fluorescence studies as well as for acid/base *in situ* studies. This instrument consists of a high-NA oil-immersion objective (Olympus, 60x, NA=1.42) mounted on an inverted focusing unit (Olympus, BXFM), with which the circularly polarized light from a continuous green diode laser (λ=532 nm, Z-laser, Z20RG) is focused onto the sample. The resulting fluorescence emission is collected by the same objective, spectrally filtered from excitation light using dichroic (Omega, 550DRLP) and long-pass (Omega, 550ALP or 600ALP) filters and finally detected in one or two avalanche photodiodes (Perkin-Elmer, SPCM-AQR-14). Under two-channel detection conditions, the emission collected by the two avalanche photodiodes was spectrally split using a dichroic filter (Omega, 600DRLP). Fluorescence images were obtained by raster-scanning micrometer-sized areas of the sample by means of a piezoscanner with position feedback control (Physik Instrumente, P-710) at 1 kHz pixelrate and with a laser excitation power density within the range 500-50 $W \cdot cm^{-2}$. The movement of the scanner as well as the collection of the signal of the photodetector is controlled by means of a LabVIEW (National Instruments) program.

Acid/base studies of DPN-patterned substrates: The DPN-patterned substrates were placed on a home-made liquid chamber and covered with 2 mL of buffer solutions of pH 3.0, 3.5, 4.0, 4.5, 5.0, 5.5, 6.0, 6.5, 7.0, 7.5, 8.0, 8.5, 9.0 and 9.5 (0.1 M), which were prepared from acetate buffer, phosphate buffer and borax buffer stock solutions. The fluorescence response of the nanostructured surfaces was then monitored by means of confocal fluorescence microscopy. High purity water was used to clean the investigated substrates between consecutive measurements.

Absorption and fluorescence measurements in solution: UV-vis absorption spectra of free OG, FL and NF dyes in solution were recorded in a HP 8452A spectrophotometer with chemstation software at defined pH values. Fluorescence emission spectra of these samples were measured by means of a

custom-made spectrofluorimeter, where a Brilliant (Quantel) pulsed laser is used as excitation source and the emitted photons are detected in an Andor ICCD camera coupled to a spectrograph. In all cases, the different protonation states of these fluorescent dyes were investigated by dissolving them in buffer solutions of the appropriate pH.

pH response of DPN-patterned substrates vs. solution: For both OG and FL DPN-patterned features, the overall change in emission intensity upon pH variation from 9.5 to 3.5 ($I_{pH=9.5}/I_{pH=3.5}$=2.0 and 5.9) is significantly lower than what is observed for those free dyes in solution at equal excitation and detection conditions ($I_{pH=9.5}/I_{pH=3.5}$=7.1 and 50 for OG and FL, respectively). As previously reported,[5] this situation should arise from the immobilization of OG and FL onto a SAM-coated glass substrate, which could cause modification of their optical properties due to interactions between close-by dye molecules as well as confinement of part of those molecules within the hydrophobic chains of the SAM, which are therefore not sensitive to the pH of the surrounding aqueous solution. As a consequence, the sensitivity of the DPN-patterned structures of OG and FL to pH changes turns to be about 5-10 times lower than in solution.

Dependence of the pH response of DPN-patterned nanostructures with deposition conditions: To investigate the effect of the DPN-patterning conditions and of the topological properties of the resulting nanostructures on their pH response, we focused our attention on one of the fluorescent dyes of interest, OG. With this aim, aminosilane SAMs were prepared onto glass slides and covalently-attached DPN-patterned structures of OG were deposited. Equivalent deposition conditions as those used to create multiplexed arrays of OG, FL and NF were applied: 35% relative humidity, 20-24 ^{o}C and dye solutions in 95% dimethylformamide and 5% glycerol. In addition, two other experimental parameters for DPN deposition were tuned (dye concentration and dwell time), and their effect on the pH response of the OG structures created was investigated by means of AFM and confocal fluorescence microscopy. In

particular, the tips for DPN-deposition were functionalized with OG solutions of two different concentrations (10 mM and 1mM) and four different dwell times were used (1 s, 0.8 s, 0.4 s and 0.1 s). Figure S3 gives the topography and friction AFM images registered for the arrays of OG structures created in this way, as well as their height cross-sections. In particular, results for 10 mM OG solutions are given in Figure S3a, while those for 1 mM OG solutions are displayed in Figure S3b. In each case, the OG structures in the array were created with different dwell times: 1 s (1st row), 0.8 s (2nd row), 0.4 s (3rd row) and 0.1 s (4th row). The average topological features (diameter and height) of those structures are given in Table S2.

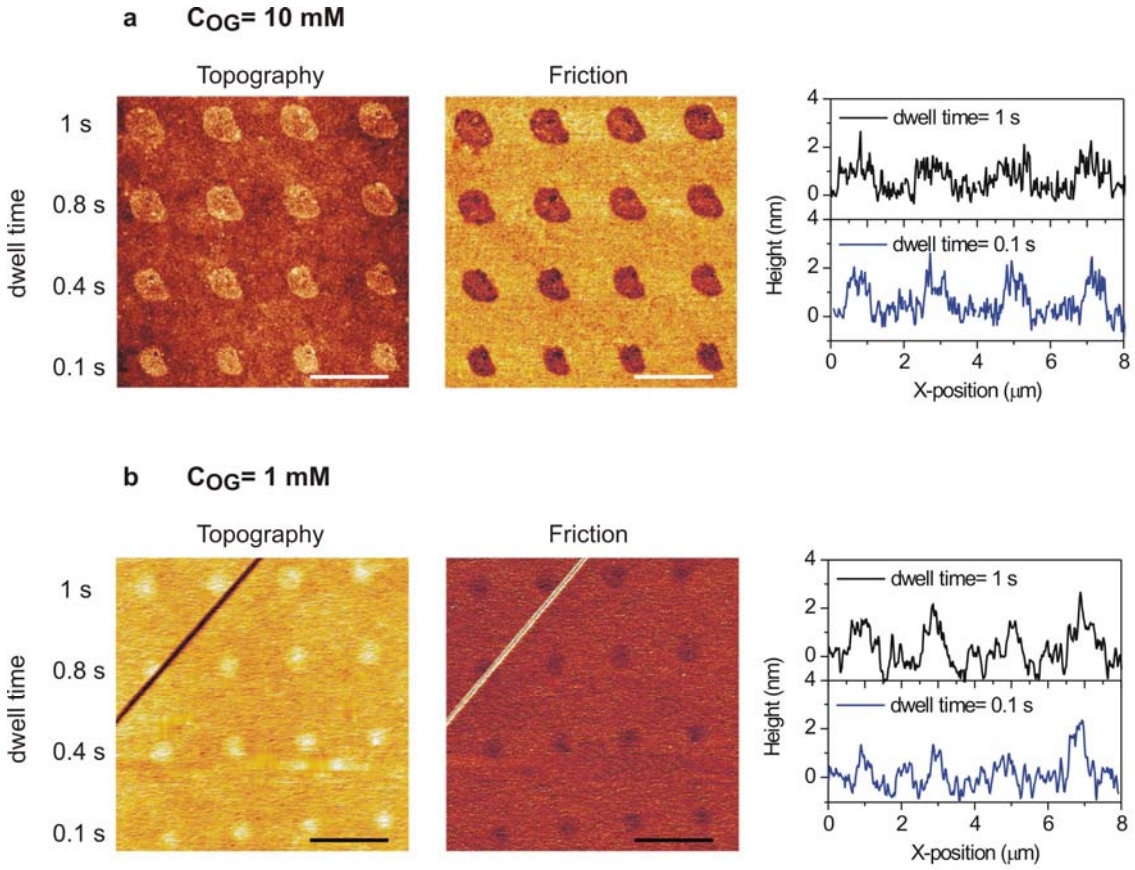

Fig. S3 Topography and friction AFM images of arrays of OG structures created by DPN from dye solutions of concentration 10 mM (a, bar= 2 μm) and 1 mM (b, bar= 2 μm). Height cross-sections of the structures in the 1st (dwell time= 1 s) and 4th (dwell time= 0.1 s) rows of the arrays are also given.

Table S2. Topological features of OG structures in Figure S3.

	C_{OG} = 10 mM		C_{OG} = 1 mM	
Dwell time [s]	Diameter [nm]	Height [nm]	Diameter [nm]	Height [nm]
1	1178 ± 88	1.45 ± 0.20	649 ± 35	1.52 ± 0.13
0.8	1022 ± 40	1.29 ± 0.19	550 ± 20	1.56 ± 0.08
0.4	858 ± 46	1.49 ± 0.11	506 ± 15	1.33 ± 0.09
0.1	740 ± 27	1.53 ± 0.24	399 ± 20	1.42 ± 0.10

All the OG structures created present a similar height (~ 1.5 nm) regardless of the experimental deposition conditions used. Such height is consistent with a monolayer of OG molecules being printed onto the surface and it confirms the removal of any residual physisorbed material resulting from deposition. On the other hand, variation of the dye concentration and dwell time results in a noticeable effect on the structure diameter, which ranges from about 1.2 μm to 400 nm. Therefore, nanometer-sized structures of fluorescent dyes can be imprinted by DPN by properly selecting the deposition conditions, as we did for the preparation of multiplexed arrays of OG, FL and NF (1 mM concentration and 0.4 s dwell time).

Figure S4a shows the confocal fluorescence image of the OG array created from a 1 mM dye solution and dwell times of 1 s (1st row), 0.8 s (2nd row), 0.4 s (3rd row) and 0.1 s (4th row), whose topography and friction AFM images are displayed in Figure S3b. The intensity cross-sections of the fluorescent features in the image are plotted in Figure S4b and their full width half-maxima (FWHM) and fluorescence intensity peaks averaged for each dwell time are given in Table S3. A clear correlation is observed between the dwell time used and the spot size and density of the resulting OG structures. As already shown by AFM measurements, the size of these structures increases with the dwell time. However, it must be noted that the lateral dimensions retrieved from the analysis of the fluorescent

features in the fluorescence image overestimate the actual sizes of the imprinted nanostructures by ~350 nm, as expected due to the limited spatial resolution of far-field optical microscopy. The intensity maxima of the fluorescent spots are also found to increase with the dwell time applied. This indicates that structures with higher density of OG molecules are created by increasing the contact time between the DPN tip and the surface. In particular, assuming a negligible effect of the dye density on optical properties, our measurements reveal that varying the dwell time from 1 s to 0.1 s for DPN deposition from a 1 mM solution of OG results in a ~30% decrease in dye density of the resulting structures.

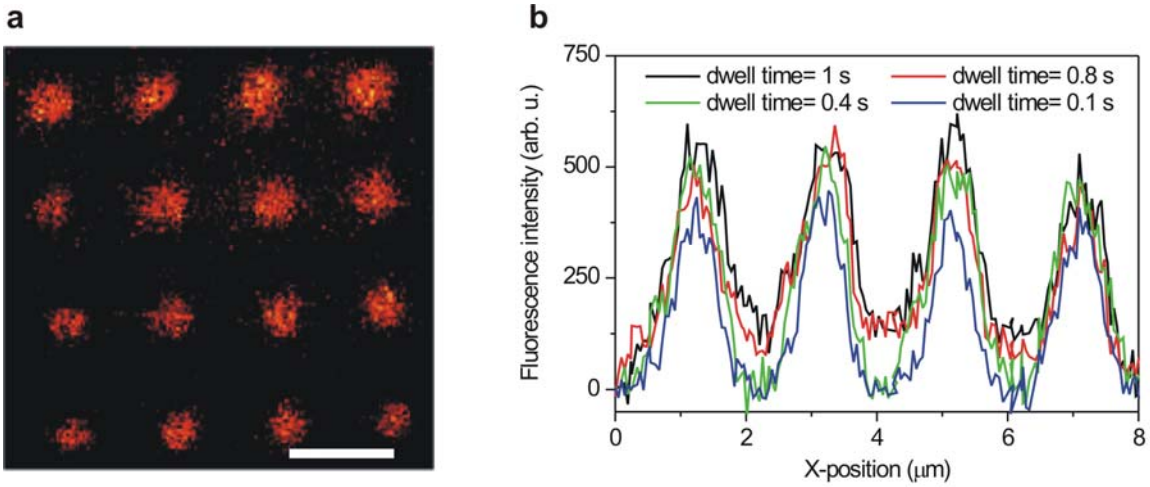

Fig. S4 (a) Confocal fluorescence image of a DPN-imprinted array of OG structures, whose topography and friction AFM images are given in Figure S3b (C_{OG}= 1 mM, dwell time= 1 s (1st row), 0.8 s (2nd row), 0.4 s (3rd row) and 0.1 s (4th row), bar= 2 μm). (b) Fluorescence intensity cross-sections of the OG structures in (a).

Table S3. Properties of the fluorescent features of OG structures in Figure S4.

	C_{OG} = 1 mM	
Dwell time [s]	FWHM[a] [nm]	Fluorescence intensity [a] [arb. u.]
1	1060 ± 85	528 ± 50
0.8	919 ± 110	487 ± 39
0.4	859 ± 56	475 ± 20
0.1	722 ± 45	389 ± 33

[a] Determined from gaussian fits of the fluorescence intensity profiles in Figure S4b.

Once proven that different deposition conditions result in OG nanopatterns with distinct structural parameters (size and density), their effect on the pH response of those nanopatterns was investigated. With this aim, the array of OG nanostructures shown in Figure S4 was exposed to buffer solutions of different pH and their fluorescence intensity measured by confocal fluorescence microscopy. Figure S5 shows the pH dependence of the average fluorescence intensity for the OG dots in this array prepared with the same dwell time. For sake of clarity, results are given normalized with respect to the fluorescence intensity at pH 7 for each dwell time value. Clearly, a sequential decrease of the fluorescence emission arising from OG structures upon acidification is observed, which follows a similar trend for all investigated dwell times, i.e. for all investigated structure sizes and densities. For instance, variation from pH 7 to pH 3 leads to relative changes in fluorescence intensity of 54%, 55%, 53% and 59% for dwell times of 1 s, 0.8 s, 0.4 s and 0.1 s, respectively. Therefore, OG structures with differences as large as 250 nm in diameter and 30% in dye density respond to pH changes with equal sensitivity. This allows us concluding that varying the size and density of the fluorescent chemosensor patterns deposited by DPN has a negligible effect on their pH response.

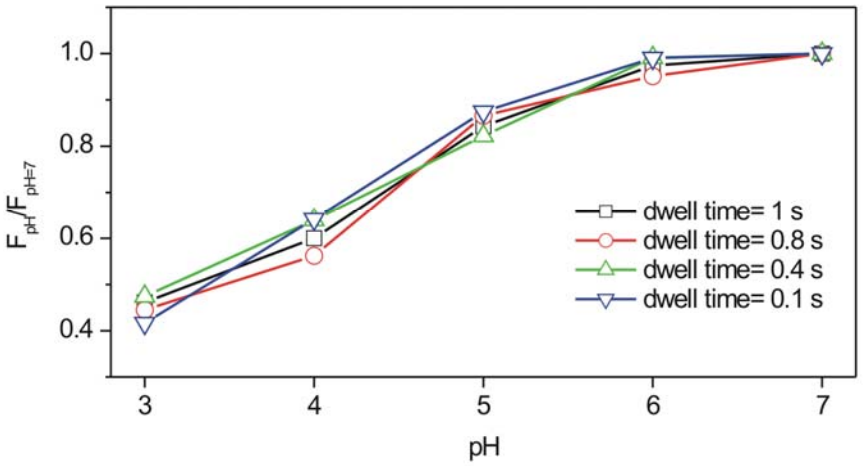

Fig. S5 pH dependence of the average fluorescence intensities of the OG structures prepared with the same dwell time in the array whose fluorescence image is shown in Figure S4. Results are given normalized with respect to the fluorescence intensity at pH 7 for each dwell time value (F_{pH} / $F_{pH=7}$).

3) References

[1] H.-J. Lin, H. Szmacinski and J. R. Lakowicz, *Anal. Biochem.* 1999, **269**, 162.

[2] R. Sjöback, J. Nygren and M. Kubista, *Spectrochim. Acta, Part A* 1995, **51**, L7.

[3] O. S. Wolfbeis, N. V. Rodríguez and T. Werner, *Mikrochim. Acta* 1992, **108**, 133.

[4] A. Hozumi, Y. Yokogawa, T. Kameyama, H. Sugimura, K. Hayashi, H. Shirayama and O. Takai, *J. Vac. Sci. Technol. A* 2001, **19**, 1812.

[5] P. Mela, S. Onclin, M. H. Goedbloed, S. Levi, M. F. García-Parajó, N. F. van Hulst, B. J. Ravoo, D. N. Reinhoudt and A. van den Berg, *Lab Chip* 2005, **5**, 163.